JOURNAL OF MATERIALS SCIENCE **36** (2001) 263–267

Sizes correction on AFM images of nanometer spherical particles

DE-QUAN YANG[a)*], YU-QING XIONG[a)], YUN GUO[a)],
DA-AN DA, WEI-GANG LU[a,b)]
[a)]*Laboratory of Applied Surface Physics, Lanzhou Institute of Physics, Chinese Academy of Space Technology, P.O. Box #94, Lanzhou 730000, People's Republic of China*
[b)]*Department of Chemistry, Lanzhou University, Lanzhou 730000, People's Republic of China*

Atomic Force Microscopy (AFM) is widely used in morphology characterization of materials on nanometer and sub-micron scales. However, distortions universally exist in AFM images due to geometrical interaction between the sample surface and the limited size tip. Correction factors for AFM images are given in the paper based on a simple mathematical model. The results reveal that the correction factors are related with the distribution of the particles (compacted or dispersed). The distortions can cause bigger images than the real sizes using commercial pyramidal tips and the distortions are deflation under certain conditions as well. The distortions of the images are affected by the shape of the AFM tip and circumstance of the particles. The results are compared the experimental data.

1. Introduction

Nanostructured materials have been paid great attention due to their novel electronic, optical, magnetic and chemical properties [1–3]. It is believed [4–6] that the properties of nanostructured materials are determined by characteristic of the crystals or particles in the materials including their sizes, shapes, and structural characters.

Atomic Force Microscopy (AFM) is a powerful tool to analysis morphology of nanostructured materials, it has been extensively used in analysis of nanocrystal thin solid films [7, 8], Langmuir-Blodgett films [9, 10], nanostructured ceramic materials [11, 12], biological materials [13, 14] and so on. AFM has the advantages of easily prepared samples and can be used in nonconductive surface analysis. But the method encounters difficulties in investigation of the morphology and structure of nanostructured materials. There are many factors affect the AFM measurements, for example, moisture on the sample surface affect the measurements due to its capillary force, the interaction between AFM tip and samples surface caused by the limited size tip [15–17]. These unwanted effects make observation of fine details of a sample surface difficult, and it significantly limits the role of the AFM for imaging features to the nanometric scale.

The sides of tip involving in image generation when the tip scans across the sample surface is illustrated in Fig. 1. It can be seen from Fig. 1 that the apparent particles size is bigger than the real particle size due to the interaction between the AFM limited size tip and the particles.

Westra *et al*. discussed the distortion of AFM images of columnar thin films caused by the finite size of the AFM tip [18]. They proposed that the ratio of the radius the curvature of the features in an AFM images to the radius of the tip provides an effective measure of the degree of tip induced distortion in an AFM image of columnar thin films.

Many mathematics models have been proposed on reconstruction of AFM images, but mainly based on the complex mathematics devolution theory [19–23]. There are many difficulties in calculation processing and semi-quantitatively relations have not been given yet. If the shape of the AFM tip is precisely known, it should be possible to reconstruct a faithful image from a distorted one [16].

In this paper, a simple mathematics model is adopted to evaluate the amount of distortion caused by limited size tip on AFM images. The discussion will be limited to the cases of spherical particles, with assumption that the tip is triangle shape [23, 24]. Correction factors for distorted morphologies are also given based on the model.

2. Theory analysis

In the paper, we assume that the shape of the pyramidal AFM tip is triangular and that of particles is spherical. The interactions between the tip and the particles are illustrated in Fig. 2. The interaction between the surface and tip is assumed to depend only on geometrical aspects [25]. The AFM tip can reach the bottom of the

* Author to whom all correspondence should be addressed.

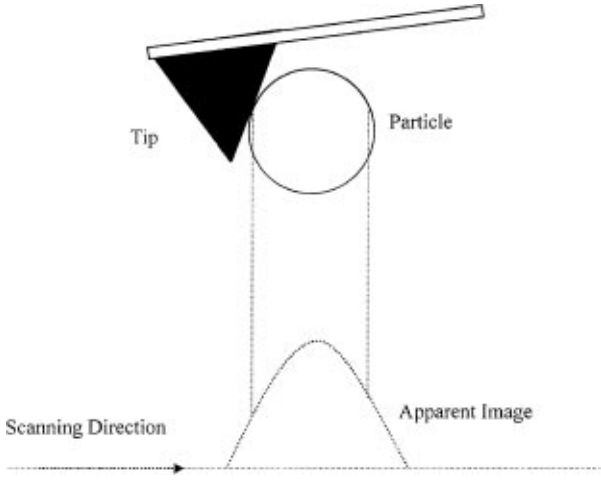

Figure 1 The interaction between the AFM tip and the particle.

particles when the distance between particles is large enough (Fig. 2a) [17], while it can not reach the bottom of the particles due to the interaction with the particles when the distance between particles is comparable with the size of AFM tip. The shape of the AFM is regarded as triangles. When the tip down to position P (Fig. 3), from geometrical operation, it is shown in Fig. 3. (see Appendix A for geometrical operation)

$$r_t = r_1 \frac{1+\sin\theta}{\cos\theta + \tan\alpha \sin\theta} = K r_1 \qquad (1)$$

Where r_t is the apparent radius, r_1 is the real size, θ is the aspect half angle of the tip, where α is a variable parameter, the meaning of α in the text is the position that the tip can reach, K is the correction coefficient.

From Equation 1, it can be seen that apparent radius of the particles are depended on the parameter (α) when the angle of the tip is given. Obviously, the tip can reach the bottom of the particles when $\alpha = 0$, at the situation r_t is maximum and expressed with r_{max}:

$$r_{max} = r_1 K_{max} \qquad (2)$$

$$K_{max} = \frac{1+\sin\theta}{\cos\theta} \qquad (3)$$

The Equation 1 confirms that the angle θ of the tip affect the investigated results directly. The effect of the angle (θ) of the tip is given in Fig. 4 according to Equation 1. From Fig. 4, it can be seen that the bigger θ is, the bigger the effect is. r_t equals to r_1 when $\theta = 0$, that is the dimension of the tip is negligible. So the angle of the tip should be one dimension at the best. The maximum correction coefficient for widely used commercial pyramidal tip ($\theta = 35^\circ$) [21] is 1.92, that is the broadening effect is 1.92 at most to this kind of tip.

Fig. 5 is the result of effect of α under a certain angle tip ($\theta = 35^\circ$). From Fig. 5, a conclusion can be drawn that $r_t = r_1$, when $\alpha = 37^\circ$, under the situation, the particles close to each other directly, the situation has been illustrated in Fig. 2b.

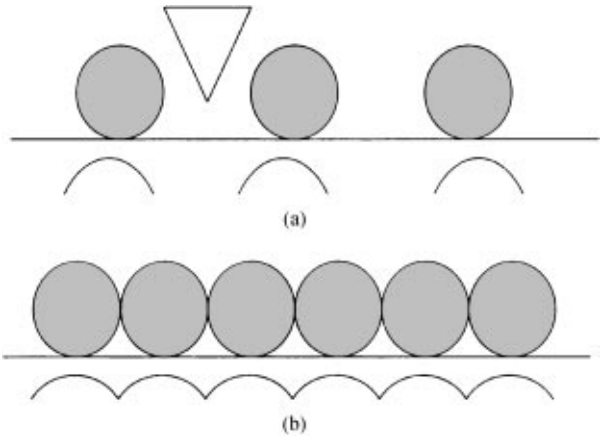

Figure 2 Interaction between the AFM tip and the particles at the surface of the specimen: (a) dispersed particles, (b) particles touching each other.

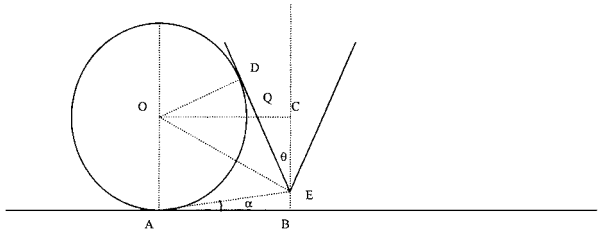

Figure 3 Mathematical model for the distortion of AFM measurement (I).

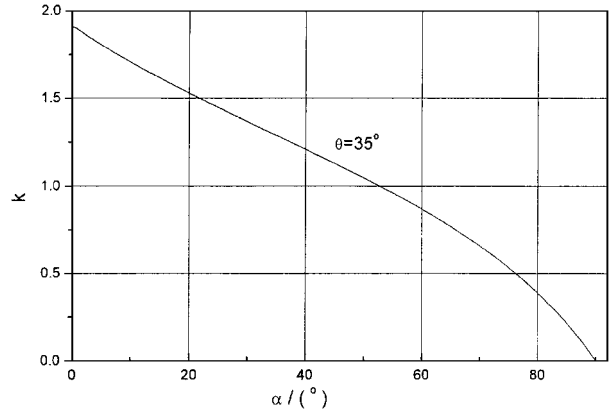

Figure 4 Effect of α on the correction coefficient.

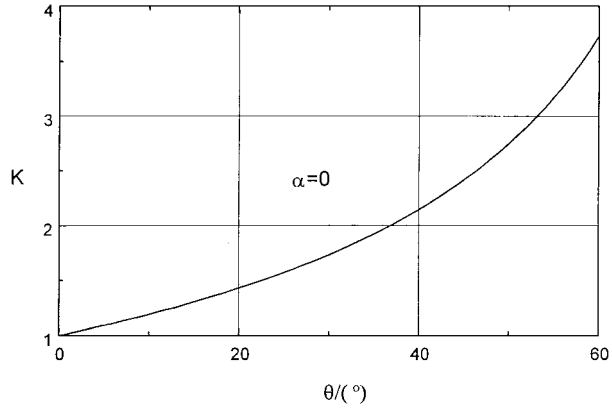

Figure 5 Effect of θ on the correction coefficient.

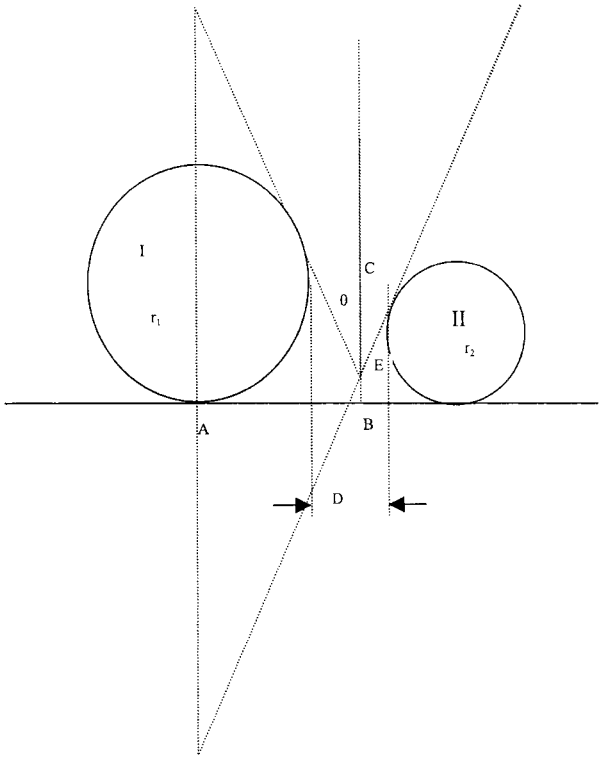

Figure 6 Mathematical model for the distortion of AFM measurement (II).

The second result of Fig. 5 is that $r_t < r_1$ also exist when α is bigger than 37°. The situation takes place when the compacted particles are not the same size. The apparent size of small particle is smaller than the real size.

The results can be expressed by another equation when the parameter is changed. As shown in Fig. 6. (Mathematics proceeding showed in Appendix B).

$$r_t = x = \left(\frac{r_1 - r_2}{2}\right)\left(\frac{1+\sin\theta}{\cos\theta}\right) + \frac{r_1 + r_2 + D}{2} = r_1 K \qquad (4)$$

Where r_t is apparent radius of particle I, r_1 is real radius of particle I, r_2 is real radius of particle II, θ is the aspect half angle of the tip, D is the distance between particle I and particle II and

$$K = 1 + \frac{D}{2r_1} + \frac{(r_1 - r_2)}{r_1}\left(\frac{1+\sin\theta}{\cos\theta} - 0.5\right) \qquad (5)$$

Where K is the correction coefficient.

The correction coefficient of Equation 5 gives effects of the angle of tip and of the size of conjoint particle (r_2) and their distance (D) as well. The effect on r_2 can also given by similar processing. The result is only suiting to the situation when the tip has not reached the bottom of the particles (the distance between particles is relatively near). The correction coefficient can be adopted the result of Equation 3 when the distance between is relatively far, when the results have no relation with the distance between the particles.

From Equation 5, it can be seen that the broadening effect is only related to the distance between particles when the close particles have the same size and it have no relation with the shape of the tip. The correction factor, K, is different when the two-impacted particle sizes are different. It is broadening effect to the big particle ($k > 1$), while it is deflation to the small one ($k < 1$). The situation also discussed in Fig. 4. In practical experimental, there is only broadening effect could be observed due to the co-effect of particles.

TABLE I Average size comparison between AFM results and other measurement methods

Sample	1#	2#	3#	4#	5#	6#
Average size of other methods (nm)	14[a)]	24[b)]	25[a)]	35[b)]	62[c)]	80[c)]
Average size of AFM (nm)	18	30.5	30	52	86.2	110.4
Ratio	1.29	1.27	1.2	1.49	1.39	1.38

a): BET results of nanoceramic powder (reference [11]); b): TEM results of nanostructured Fe_2O_3 particles obtained in our laboratory; c): XRD result of nanoceramic powder (reference [12]).

3. Results and discussion

Table I is results comparison of different size particles between AFM and other measurement methods. The particle size of TEM of our lab was estimated by counting 100 particles to represent all, AFM size were obtained by counting 100 particles on the profiles line, the AFM tip used in our experimental was commercial pyramidal tip ($\theta = 35°$). From Table I, it can be seen that the size obtained by AFM has broadening effect comparison with other methods, and the difference is within prediction of our theory.

As mentioned above, the results of AFM can be corrected with a correction coefficient (K). The value of K is usually in the range of 1.0–1.92. The average value 1.46 can be used as a common correction coefficient to reconstruct the apparent size of spherical particles obtained by AFM, that is the experimental result divided by 1.46 should be the real size of the investigated particles.

Of course, if a tip with larger θ is used, the correction coefficient maybe vary different, for example, if $\theta > 37°$, the value of K will be larger than 2, this is the case of reference [26].

4. Conclusion

The geometrical interaction between AFM limited size tip and sample surface can cause the apparent results distortion compare with the real surfaces. The distortions related with the shape of AFM, the distribution of particles sizes and cumulate conditions of the particles. The correction coefficient is usually between the range 1.0–1.92. Suitable coefficient can be adopted under different experimental conditions.

Appendix A

As showed in Fig. 3 it can be seen from geometrical relationship

$$\Delta \mathrm{ODQ} \sim \Delta \mathrm{QCE}$$

Apparent radius AB = OC, while

$$\mathrm{OC} = \mathrm{OQ} + \mathrm{QC} = r_\mathrm{t}$$
$$\mathrm{OQ} = \frac{r_1}{\cos\theta}, \quad \mathrm{QC} = \mathrm{CE}\tan\theta \tag{A1}$$

Where r_t is the apparent radius, r_1 is the real size, θ is the aspect half angle of the tip.

We assume $\angle \mathrm{BAC} = \alpha$, where α is a variable parameter, the meaning of α in the text is the position that the tip can reach

$$r_1 = \mathrm{BE} + \mathrm{EC}$$
$$\mathrm{BE} = r_\mathrm{t}\tan\theta \tag{A2}$$
$$\mathrm{EC} = r_1 - \mathrm{BE} = r_1 - r_\mathrm{t}\tan\alpha \tag{A3}$$

So

$$r_\mathrm{t} = \frac{r_1}{\cos\theta} + \mathrm{EC}\tan\theta \tag{A4}$$
$$\mathrm{EC} = \frac{r_\mathrm{t} - \frac{r_1}{\cos\theta}}{\tan\theta} \tag{A5}$$

from (A4), (A5):

$$r_1 - r_\mathrm{t}\tan\alpha = \frac{r_\mathrm{t} - \frac{r_1}{\cos\theta}}{\tan\theta} = \frac{r_\mathrm{t}\cos\theta - r_1}{\sin\theta} \tag{A6}$$

Simplifying (A6):

$$r_\mathrm{t} = r_1\frac{1+\sin\theta}{\cos\theta + \tan\alpha\sin\theta} = Kr_1 \tag{A7}$$

Where K is the correction coefficient.

Appendix B

As shown in Fig. 6, We let A as zero, AB as x-axis, AO as y-axis. The slope of the tangible line of the bigger circles equals to $\tan(90^\circ + \theta)$, intercept is $r_1 + \frac{r_1}{\sin\theta}$, so tangential equation is

$$y = \tan(90^\circ + \theta)x + \left(r_1 + \frac{r_1}{\sin\theta}\right) \tag{B1}$$

Where r_1 is the real size of particle I,θ is the aspect half angle of the tip.

Coequally, the intercept of the small circle's tangent is $\tan(90^\circ - \theta)$, intercept is $r_1 + \frac{r_1}{\sin\theta}$, so the tangential equation is

$$y = \tan(90^\circ - \theta)[x - (r_1 + r_2 + D)] + \left(r_2 + \frac{r_2}{\sin\theta}\right) \tag{B2}$$

Where r_2 is radius of particle II, D is the distance between particle I and particle II (see Fig. 6). So point of intersection of the both tangent equals to:

$$\tan(90^\circ + \theta)x + \left(r_1 + \frac{r_1}{\sin\theta}\right) = \tan(90^\circ - \theta)[x - (r_1 + r_2 + D)] + \left(r_2 + \frac{r_2}{\sin\theta}\right) \tag{B3}$$

In short:

$$r_\mathrm{t} = x = \left(\frac{r_1 - r_2}{2}\right)\left(\frac{1+\sin\theta}{\cos\theta}\right) + \frac{r_\mathrm{t} + r_2 + D}{2} = r_1 K \tag{B4}$$

Where r_t is apparent radius of particles I

$$K = 1 + \frac{D}{2r_1} + \frac{(r_1 - r_2)}{r_1}\left(\frac{1+\sin\theta}{\cos\theta} - 0.5\right) \tag{B5}$$

is the correction coefficient.

References

1. G. C. HADJIPANAYIS and R. W. SIEGEL (eds.), "Nanophase Materials" (Kluwer Academic Publishers, Netherlands 1994).
2. R. L. HOLTZ, V. PROVENZANO and M. A. IMAM, *Nanostructured Materials* **7** (1996) 259.
3. M. L. TRUDEAU and J. Y. YING, *ibid.* **7** (1996) 245.
4. P. MARGUARDT, I. BORNGEN, G. NIMTZ, R. SONNBERGER, H. GLEITER and J. ZHU, *Phys. Lett.* **114A** (1986) 39.
5. R. F. ZLOLO, E. P. GLANNELLS, B. A. WELNSEIN, M. P. OHORO, B. N. GANULY, V. MRHROTRA, M. W. RUSSELL and D. R. HUFFMAN, *Science* **257** (1992) 219.
6. S. JIN, T. H. TIEFEL, M. MCORMACK, R. RAMESH and L. CHEN, *ibid.* **264** (1994) 413.
7. Y. SASAKI, K. SHIOZAWA, H. TANIMOTO, Y. IWAMOTO, E. KITA and A. TASAKI, *Mater. Sci. Eng. A* **217/218** (1996) 344.
8. H. TANIMOTO, H. FUJITA, H. MIZUBAYASHI, Y. SASAKI, E. KITA and S. OKUDA, *ibid.* **217/218** (1996) 108.
9. J. A. DEROSE and R. M. LEBLANO, *Surf. Sci. Reports* **22** (1995) 73.
10. D. Q. YANG, Y. SUN, Y. GUO, R. F. WANG, S. P. XIE and D. A. DA, *Phys. Stat. Sol. B* **203** (1997) R7.
11. A. DIAS, R. L. MOREIRA, N. D. S. MOHALLEN, J. M. C. VILELA and M. S. ANDRADE, *J. Mater. Res.* **13** (1998) 223.
12. A. DIAS, V. T. L. BUONO, J. MC. VILELA, MS. ANDRADE and T. M. LIMA, *J. Mater. Sci.* **32** (1997) 4715.
13. C. BUATAMANTE and D. KELLER, *Phys. Today* **32** (1995) 3.
14. H. G. HANSMA and H. J. HOH, *Annu. Rev. Biophys. Biomol. Struct. B* **23** (1994) 115.
15. C. J. ROBERTS, M. J. WILKINS, G. BEAMSON, M. C. DAVIES, D. E. JACKSON, P. D. SCHOLES, S. J. B. TENDLER and P. M. WILLIAMS, *Nanotechnology* **3** (1992) 98.
16. D. J. KELLER, *Surf. Sci.* **253** (1991) 353.
17. D. J. KELLER and F. S. FRANKE, *ibid.* **294** (1993) 409.
18. K. L. WESTRA and D. J. THOMSON, *J. Vac. Sci. Thehnol. B* **13** (1995) 344.

19. R. CHICON, M. ORTUNO and J. ABLLAN, *Surf. Sci.* **181** (1987) 107.
20. P. MARKIEWICZ and M. C. GOH, *Langmuir* **10** (1994) 5.
21. D. L. WILSON, K. S. KUMP, S. J. EPPELL and R. E. MARCHANT, *ibid.* **11** (1995) 265.
22. E. C. W. LEUNG, P. MARKIEWICZ and M. C. GOH, *J. Vac. Sci. Technol. B* **15** (1997) 181.
23. P. M. WILLIAMS, K. M. SHAKESHEFF, M. C. DAVIES, D. E. JACKSON, C. J. ROBERTS and S. J. B. TENDLER, *Langmuir* **12** (1994) 3468.
24. Omicron SPM Manual.
25. S. S. SHEIKO, M. MILLER, E. M. C. M. REUVEKAMP and H. W. ZANDBERGEN, *Phys. Rev. B* **48** (1993) 5675.
26. H. TANIMOTO, H. FUJITA, H. MIIZUBAYASHI, Y. SASAKI, E. KITA and S. OKUDA, *Mater. Sci. Eng. A* **217/218** (1996) 108.

Received 17 March 1999
and accepted 24 April 2000